PERGAMON

International Journal of Solids and Structures 37 (2000) 2429–2442

INTERNATIONAL JOURNAL OF SOLIDS and STRUCTURES

www.elsevier.com/locate/ijsolstr

Connection between interface corner and interfacial fracture analyses of an adhesively-bonded butt joint

E.D. Reedy Jr*

Sandia National Laboratories, Albuquerque, NM 87185, USA

Received 21 July 1998; in revised form 6 December 1998

Abstract

Interfacial crack growth in a tensile-loaded, adhesively-bonded butt joint with rigid adherends is analyzed. First, the asymptotic, small-scale cracking solution for a short interfacial crack originating at a sharp interface corner is presented. Then the asymptotic, steady-state solution for a long interfacial crack is discussed. These asymptotic results are compared with full finite element solutions of a butt joint containing a 0.001 to 10 bond thickness long interfacial crack. Finally, the applicability of both interface corner and interfacial fracture mechanics approaches to failure analysis is discussed. The small-scale cracking solution indicates that when one can apply an interface corner failure analysis, one can also apply an interfacial fracture mechanics approach with a suitably chosen inherent flaw. Although the two methods are equivalent, it should be emphasized that the inherent flaw and corresponding toughness may have limited physical significance. Published by Elsevier Science Ltd.

Keywords: Adhesive; Bond; Corner; Fracture; Interface; Joint; Strength

1. Introduction

The connection between two different approaches for analyzing the fracture of an adhesively-bonded butt joint is examined. This type of joint is commonly used to evaluate adhesives and also presents a convenient geometry to analyze. Here an idealized butt joint with rigid adherends and a thin, essentially semi-infinite, bond is analyzed (Fig. 1). This idealization is applicable when the adherends are much stiffer than the adhesive (e.g. steel adherends and epoxy adhesive), and when the bond thickness is much smaller than any other joint dimension.

In a noteworthy study Anderson and DeVries (1987, 1989) use a linear elastic fracture mechanics approach to analyze adhesively-bonded butt joints. They assume that the joint behaves as if a characteristic, inherent flaw is present and suggest that inherent flaws may be related to those that exist naturally in all

* Fax: +1-505-844-9297.
E-mail address: edreedy@sandi.gov (E.D. Reedy, Jr)

0020-7683/00/$ - see front matter. Published by Elsevier Science Ltd.
PII: S0020-7683(99)00002-5

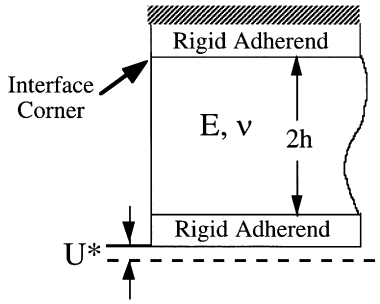

Fig. 1. Tensile-loaded, adhensively-bonded butt joint with rigid adherends.

bonds due to such things as air bubbles, local surface discontinuities, etc. Consequently, their approach requires the determination of a critical toughness value, G_c, and also an inherent flaw size, a_0. This is done by first measuring G_c using joints with intentionally inserted interfacial disbonds of known size. Joints without inserted disbonds are also tested. The energy release rate vs crack length calibration (i.e., G vs a relationship) for the butt joint test geometry is then used to determine the a_0 value that is consistent with the strength of the joints without inserted disbonds and $G = G_c$. Employing these G_c and a_0 values, the authors were then able to successfully predict the dependence of butt joint strength on bond thickness.

In more recent work Reedy and Guess (1993, 1995, 1997) have used a method based upon the stress intensity factor associated with an interface corner (the point where the interface intersects the stress-free edge, Fig. 1) to predict the failure of adhesively-bonded butt joints. When viewed asymptotically, the interface corner is at the apex of a multi-material wedge. It is well known that within the context of linear elasticity theory, a stress singularity of type

$$\sigma \sim K_a r^{\delta} \quad (\delta < 0) \tag{1}$$

can exist at an interface corner (Williams, 1952; Bogy, 1968, 1970). Note, that this subscript 'a' on K in eqn (1) is used to denote that this stress intensity factor is associated with the apex of a wedge. The value of the stress intensity factor K_a characterizes the magnitude of the stress state in the region of the interface corner. The calibration relation defining K_a is determined by the full solution, and it depends on loading, geometry, and elastic properties. There has been a recent emphasis on determining K_a relations for geometries and loadings of practical importance (Akisanya and Fleck, 1997; Chen, 1994; Ding et al., 1994; Munz and Yang, 1992; Reedy, 1990; Reedy and Guess, 1997; Szabó and Yosibash, 1996). It appears reasonable to hypothesize that failure occurs at a critical K_a value. Such an approach is analogous to linear elastic fracture mechanics except here the critical K_a value is associated with a discontinuity other than a crack. Several experimental studies have investigated a failure analysis based on a critical K_a value (Gradin, 1982; Groth, 1988; Hattori et al., 1989; Reedy and Guess, 1993, 1995, 1997). As is the case of linear elastic fracture mechanics, small-scale yielding conditions must apply. The asymptotic stress state characterized by K_a must dominate a region that is significantly larger than the fracture process zone, plastic yield zone, and the extent of any subcritical cracking. The corner must also appear sharp when viewed at this length scale. The interface corner stress intensity factor approach for adhesively-bonded butt joints requires the determination of a single fracture parameter, the interface corner toughness K_{ac}. This is done by measuring joint strength at one bond thickness. This joint strength is used in conjunction with the calculated K_a calibration relationship to determine the critical K_a value, K_{ac}. This method has successfully predicted the variation of strength of adhesively-bonded butt joints with bond thickness as well as the dependence of this relationship on adherend stiffness (Reedy and Guess, 1993, 1997). It is noted that a similar approach has also been used by Dunn et al. (1997a, b) to successfully predict the fracture of a homogenous material containing a sharp notch.

This paper examines the connection between interface corner and interfacial fracture analyses of an adhesively-bonded butt joint with rigid adherends. First, asymptotic solutions for both short and long interfacial cracks originating at a sharp interface corner are presented. These asymptotic results are then compared with full finite element solutions to investigate their range of applicability. Finally, the applicability of both interface corner and interfacial fracture mechanics approaches to failure analysis is discussed.

2. Asymptotic solutions

This section begins with a brief review of those interfacial fracture and interface corner analysis results used in the asymptotic solutions that follow. These plane strain results are specialized to the case where the upper adherend is rigid (material 1 in Fig. 2). When the upper material is rigid, the elastic mismatch parameters (Dundurs, 1969) are

$$\alpha = 1$$
$$\beta = \frac{1-2\nu}{2(1-\nu)} \tag{2}$$

2.1. Interface corner analysis

The stress intensity factor associated with the singular stress field surrounding the interface corner in an adhesively-bonded butt joint with rigid adherends has been determined by Reedy (1990). The adhesive layer is assumed to be isotropic and linear elastic. Directly in front of the interface corner (Fig. 1), the traction normal to the interface is

$$\sigma_{yy} = K_a r^{\lambda-1} \tag{3}$$

where r = distance from the interface corner; $\lambda - 1$ = order of the stress singularity (depends only on ν); and K_a = interface corner stress intensity factor. For a tensile-loaded, adhesively-bonded butt joint with rigid adherends and a thin (essentially semi-infinite) adhesive layer

$$K_a = \sigma^* h^{1-\lambda} A_p(\nu) \tag{4}$$

where the characteristic stress σ^* is related to the nominal applied tensile stress $\bar{\sigma}$ by

$$\sigma^* = \left(\frac{\nu}{1-\nu}\right)\bar{\sigma}. \tag{5}$$

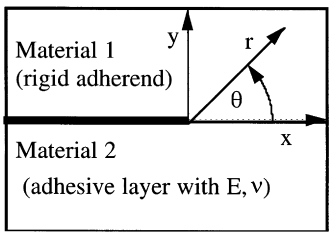

Fig. 2. Conventions used to define interfacial crack configuration.

Table 1
Parameters defining the small-scale cracking solution for tensile-loaded, adhesively-bonded butt joints with rigid adherends

ν	β	$1-\lambda$	$A_p(\nu)$	$D(\nu)$	$\hat{\psi}_{r=a}$ (degrees)
0.05	0.474	0.077	14.70	4.26	−12.3
0.10	0.444	0.133	6.63	4.51	−13.5
0.15	0.412	0.179	3.96	4.75	−14.4
0.20	0.375	0.219	2.63	5.00	−15.1
0.25	0.333	0.255	1.84	5.26	−15.7
0.30	0.286	0.289	1.32	5.55	−16.2
0.35	0.231	0.320	0.958	5.89	−16.5
0.40	0.167	0.350	0.654	6.30	−16.7
0.45	0.091	0.378	0.391	6.81	−16.7

and A_p is a function of ν only. A_p and $1-\lambda$ values are listed in Table 1 for a wide range of ν. When $\nu = 0.35$, $1-\lambda = 0.320$, and $A_p = 0.958$. Note that this A_p value is the one reported in Reedy and Guess (1997). This value was determined using a more highly refined finite element mesh than that used in Reedy (1990) and is 1% higher than reported earlier. As an aside, the K_a relation defined by eqn (4) is also applicable to a transversely cracked elastic layer that is sandwiched between rigid layers (assuming a single, isolated crack). The stress-free edge can be considered a symmetry plane when the bounding layers are rigid.

2.2. Interfacial fracture mechanics

The singular stress state at the tip of a crack lying on the interface between two dissimilar, linear-elastic, isotropic materials is well known (Rice, 1988; Hutchinson and Suo, 1992). The interfacial tractions directly ahead of the crack tip (Fig. 2) are given by

$$\left(\sigma_{yy} + i\sigma_{xy}\right)_{\theta=0} = \frac{Kr^{i\varepsilon}}{\sqrt{2\pi r}} \tag{6}$$

where

$$K = K_1 + iK_2, \quad i \equiv \sqrt{-1} \quad \text{and} \quad \varepsilon = \frac{-\ln(3-4\nu)}{2\pi}$$

Furthermore, the energy release rate G for crack advance along the interface is related to the complex interfacial stress intensity factor by

$$G = \frac{1-\beta^2}{E^*}|K|^2 \tag{7}$$

where

$$E^* = \frac{2E}{(1-\nu^2)} \quad \text{and} \quad |K|^2 = K_1^2 + K_2^2$$

A generalized interpretation of mode measure has been suggested by Rice (1988), and this definition is now widely used. Mode mixity $\hat{\psi}$ is defined as the ratio of interfacial shear stress to normal stress at a

fixed distance $\hat{l}$ in front of the crack tip.

$$\hat{\psi}_{r=\hat{l}} = \tan^{-1}\left[\left(\frac{\sigma_{xy}}{\sigma_{yy}}\right)_{\theta=0,r=\hat{l}}\right] = \tan^{-1}\left[\frac{\mathrm{Im}\left(K\hat{l}^{i\varepsilon}\right)}{\mathrm{Re}\left(K\hat{l}^{i\varepsilon}\right)}\right] \tag{8}$$

The choice of reference length $\hat{l}$ is arbitrary and is sometimes based on a characteristic inplane length of the body analyzed or on an intrinsic material length scale. In any case, $\hat{\psi}$ values corresponding to two different length scale $\hat{l}_1$ and $\hat{l}_2$ are related by

$$\psi_{r=\hat{l}_2} = \psi_{r=\hat{l}_1} + \varepsilon \ln\left(\hat{l}_2/\hat{l}_1\right) \tag{9}$$

2.3. Small-scale cracking

The small-scale interfacial cracking problem for a crack originating at an interface corner is completely analogous to the small-scale yielding problem of traditional fracture mechanics. In recent work Akisanya and Fleck (1997) and Grenestedt and Hallstrom (1997) have considered such problems. A short, interfacial crack is considered to be fully embedded within the region dominated by the interface corner stress singularity (Fig. 3). The angular variation of displacements along the outer boundary ($r \gg a$) is known from the interface corner solution, and K_a determines the magnitude of the loading. In accordance with linear elasticity, $|K|$ for the interfacial crack must depend linearly on K_a. The only length scale in this asymptotic problem is crack length a, and the only nondimensional parameter that exists, or can be formed, is ν. Consequently, to be dimensionally correct, energy release rate must depend on crack length and K_a as

$$G = \frac{\left(1-\beta^2\right)}{E^*}|K|^2 = \frac{\left(1-\beta^2\right)}{E^*}K_a^2 a^{2\lambda-1} D(\nu) \tag{10}$$

Dimensional considerations require that mode mixity $\hat{\psi}_{r=a}$ is also only a function of ν. $D(\nu)$ and $\hat{\psi}_{r=a}$ are determined by solving the asymptotic problem for ν values of interest. The G relation defined by eqn (10) can be specialized to the case of a tensile-loaded, adhesively-bonded butt joint by substituting the K_a relationship for that geometry and loading (eqn (4)).

$$G = \frac{\left(1-\beta^2\right)}{E^*}h^{2(1-\lambda)}a^{2\lambda-1}A_p(\nu)^2 D(\nu)\sigma^{*2} \tag{11}$$

or equivalently

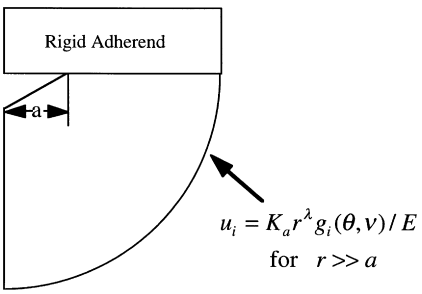

Fig. 3. Small-scale cracking problem.

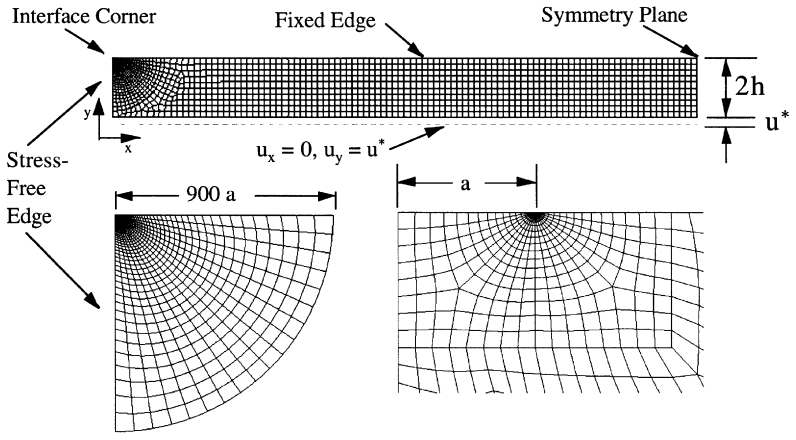

Fig. 4. Typical finite element mesh used in adhesively-bonded butt joint analysis as well as the portion used in small-scale cracking analysis.

$$G = \frac{(1-\beta^2)}{E^*}\left(\frac{\nu}{1-\nu}\right)^2 A_p(\nu)^2 D(\nu)\left(\frac{h}{a}\right)^{1-2\lambda}\bar{\sigma}^2 h \tag{12}$$

When $\nu = 0.35$, $\lambda \sim 2/3$. Eqn (11) indicates that when small-scale cracking conditions exist, G for an adhesively-bonded butt joint with rigid adherends varies as $h^{2/3}$ and as $a^{1/3}$.

Table 1 lists $D(\nu)$ and mode mixity $\hat{\psi}_{r=a}$ values for a broad range of ν. These values were determined by carrying out a plane strain, finite element analysis of the asymptotic problem for each ν using the quarter circle mesh shown in Fig. 4. The outer boundary is at a radius of $900a$ and is loaded by the asymptotic, interface corner displacement field that corresponds to the prescribed ν. The mesh is composed of eight-noded, isoparametric quadrilateral elements. The wedge-shaped elements that surround the crack tip are formed by collapsing one side of quadrilateral elements. The collapsed, crack tip nodes are constrained to have the same displacement, whereas the mid-side nodes closest to the crack tip are moved to the quarter-point position to incorporate a square root singularity. The length of the smallest element is roughly 0.000004 of the adhesive bond thickness. The energy release rate is determined by a J-integral evaluation, whereas mode mixity $\hat{\psi}_{r=a}$ is calculated using crack flank displacements (Matos et al., 1989). Note that the reported $D(\nu)$ apply not only to the adhesively-bonded butt joint but also to any problem where the asymptotic problem is a quarter plane with one edge fixed and the other edge stress-free (e.g., debonding at the tip of a transverse crack in a thin layer on a rigid substrate). Eqn (10) relates G to any existing K_a relation.

2.4. Steady-state cracking

The energy release rate for the long crack, steady-state asymptotic problem is readily determined via a J-integral evaluation (Rice, 1968)

$$G_{ss} = \frac{(1+\nu)(1-2\nu)}{(1-\nu)E}\bar{\sigma}^2 h \tag{13}$$

A finite element solution for a geometry approximating the long crack limit indicates $\hat{\psi}_{r=2h} = -16.4^0$ when $\beta = 0.231$.

3. Comparison with full finite element solutions

To provide a focus for the calculations presented below, the specimen geometry, material properties, and failure load are drawn from a previously reported test series (Reedy and Guess, 1993). These joints were fabricated by bonding two, 28.6 mm diameter stainless steel rods together with an Epon 828/T-403 epoxy adhesive (100/36 by weight mix ratio, cured at room temperature). This epoxy's Young's modulus $E = 3.5$ GPa and Poisson's ratio $\nu = 0.35$. The bond thickness of the joints was varied from 0.25 mm to 2.0 mm. The measured variation in strength with bond thickness is consistent with a critical interface corner stress intensity factor value $K_{ac} = 12.7$ MPa mm$^{0.32}$. With this value of K_{ac}, a joint with a 1.0 mm adhesive layer fails at a nominal tensile load of 30.7 MPa.

A full, finite element analysis of an adhesively-bonded butt joint with rigid adherends has been carried out to investigate the range of applicability of the asymptotic solutions. Fig. 4 shows a typical finite element model. The upper edge of the adhesive layer is fixed, whereas the lower edge is displaced downward. The right-hand edge is a symmetry plane. The model contains an interfacial crack originating at the upper interface corner with a crack length that ranges from 0.001 to 10 times the bond thickness. As indicated in Fig. 4, the same sort of highly refined quarter circle mesh, as used in the small-scale cracking asymptotic analysis, is used in the full joint analysis. The uncracked portion of the joint is 20 h long to ensure that stress at the symmetry plane is unaffected by the presence of the stress-free edge (i.e., models a semi-infinite bond).

Fig. 5 illustrates the nature of the small-scale cracking problem when $a = 0.01$ mm and $2h = 1.0$ mm. Asymptotic interface corner and small-scale cracking solutions for interfacial normal stress are compared to finite element results for the full joint model. The interface corner stress solution is defined by eqns (3)–(5). Note that the reason the plotted curve on this log-log plot is not a straight line is because stress is plotted as a function of distance from the crack tip, not distance from the interface corner. The small-scale cracking result is obtained by using eqn (12) and the phase angle listed in Table 1 to determine the complex interfacial stress intensity factor using eqns (7–9). The interfacial normal stress is then calculated using eqn (6). The small-scale cracking solution merges with the full joint solution at a distance of $<.01$ mm. At a distance of 0.01 mm in front of the crack-tip (a distance equal to the crack length), the small-scale cracking solution is within 10% of the full-joint model solution. The stress field associated with the interface crack is embedded within the field governed by the interface

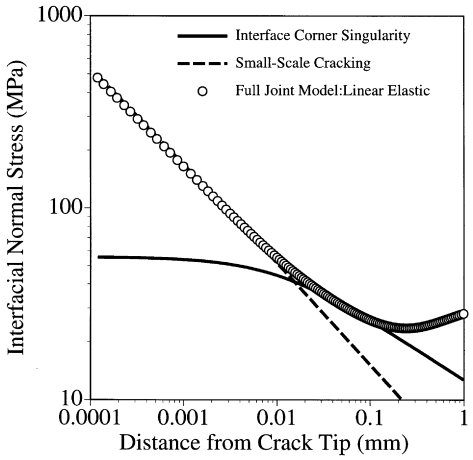

Fig. 5. Comparison of asymptotic interface corner and small-scale cracking solutions for interfacial normal stress with finite element resutls for the full joint model ($a = 0.01$ mm, $\bar{\sigma} = 30.7$ MPa).

Table 2
Comparison of finite element and asymptotic solutions for energy release rate ($\bar{\sigma} = 30.7$ MPa). G_{FEA} is the finite element solution; G_{asym} is the small-scale cracking solution; and G_{ss} is the long crack, steady-state solution

$2h$ (mm)	a (mm)	G_{FEA} (J/m^2)	G_{asym} (J/m^2)	G_{FEA}/G_{asym}	G_{FEA}/G_{ss}
1.0	0.001	9.1	9.4	0.97	0.11
1.0	0.010	20.5	21.4	0.96	0.24
1.0	0.100	42.8	49.1	0.87	0.51
1.0	0.500	70.2	87.7	0.80	0.84
1.0	1.000	80.9	112.5	0.72	0.96
1.0	10.00	84.1	257.7	0.33	1.00
2.0	0.001	14.2	14.6	0.97	0.08
2.0	0.010	32.3	33.4	0.97	0.19

corner singularity. Once beyond the region perturbed by the interface crack, the interface corner singularity and the full-joint model solutions are within 10% out to a distance of 0.15 mm (15% of the total bond thickness).

Table 2 compares the calculated energy release rate using the full joint model (G_{FEA}) with the asymptotic solutions for small-scale cracking (G_{asym}) and steady-state cracking (G_{ss}) over a broad range of crack lengths. Most results are for a 1-mm thick bond, although a couple of calculations are for a 2-mm thick bond. These later results provide an additional confirmation of the scaling implied by the small-scale cracking solution. The results for the 1-mm thick bond are plotted in Fig. 6. Together the asymptotic solutions form a fairly tight envelope of G_{FEA} over the full range of crack lengths. The small-scale cracking solution is within a few percent of G_{FEA} for $a/h < .02$ and differs by 20% at $a/h = 1$. The steady-state cracking solution is within a few percent of G_{FEA} for $a/h > 2$ and differs by 16% at $a/h = 1$. Fig. 7 plots a similar comparison for mode mixity. Here the phase angle is defined at a characteristic length scale of 0.01 mm (as shown below, this is on the order of the interface corner yield zone). Again, the asymptotic solutions form a fairly tight envelope of the phase angle calculated using

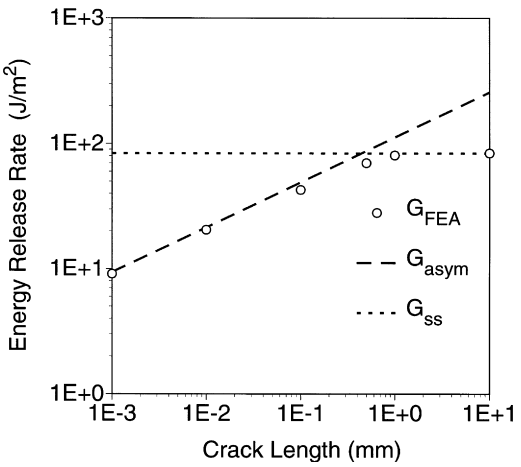

Fig. 6. Comparison of finite element and asymptotic solutions for energy release rate ($\bar{\sigma} = 30.7$ MPa). G_{FEA} is the finite element solution; G_{asym} is the small-scale cracking solution; and G_{ss} is the long crack, steady-state solution.

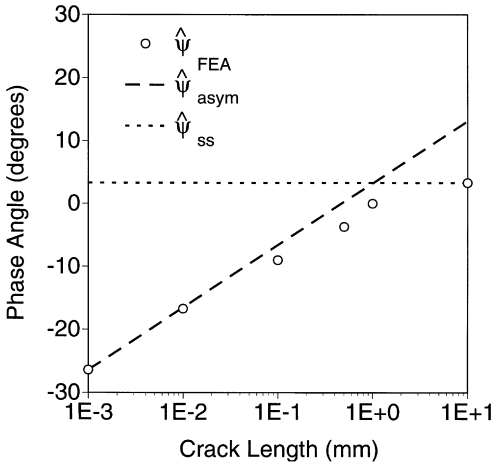

Fig. 7. Comparison of finite element and asymptotic solutions for $\hat{\psi}_{r=0.01\ mm}$. $\hat{\psi}_{FEA}$ is the finite element solution; $\hat{\psi}_{asym}$ is the small-scale cracking solution; and $\hat{\psi}_{ss}$ is the long crack, steady-state solution.

the full joint model. Note that the phase angle starts out negative, and increases steadily until it is slightly positive. Consequently, an interfacial crack might be pushed away from the interface as it grows. This is consistent with butt joint test results (Reedy and Guess, 1993). In these tests fracture initiated on the interface along a small segment of the specimen periphery. As the crack grew, it moved off of the interface, and fracture occurred within the adhesive layer.

4. Applicability to failure analysis

One can envision using either an interface corner or an interfacial fracture analysis to predict the failure of adhesively-bonded butt joints. Under certain conditions there should even be a direct connection between the fracture parameters used in the two approaches. There are, however, restrictions in the applicability of both techniques.

An interface corner failure analysis is applicable when unstable crack growth initiates from a fracture process zone that is deeply embedded within the region dominated by the interface corner signularity. The size of the region dominated by the stress singularity can be estimated by comparing finite element results for the full joint model with the singularity solution. This size estimate depends to some degree on which stress measure is compared, as well as the angular position considered. For rigid adherends and an epoxy adhesive bond, effective stress along a ray bisecting the interface corner ($\theta = -\pi/4$) is in good agreement with the singular solution out to 30% of the bond thickness, whereas interfacial mean stress is in good agreement out to 15% of the bond thickness (Reedy, 1993, also see Fig. 5). Consequently, not only must the corner appear sharp when viewed at this length scale, but also material yielding and subcritical crack growth must be limited to a few percent of the total bond thickness.

The size of the interface corner fracture process zone is not known. Indeed there is no detailed information on the fracture process. One can, however, estimate the extent of yielding. Fig. 8 shows three different predictions for the interface corner yield zone at joint failure. These results are for a joint with no interface crack. Note as was indicated earlier, the failure load and epoxy properties, used in all calculations are based on a previously reported series of steel/epoxy butt joint tests (i.e., $K_{ac} = 12.7$ MPa $mm^{0.32}$, $\bar{\sigma} = 30.7$ MPa, $2h = 1.0$ mm). Epoxy yielding is rate and temperature dependent and is thought to be a manifestation of stress-dependent, nonlinear viscoelastic material response. Unfortunately,

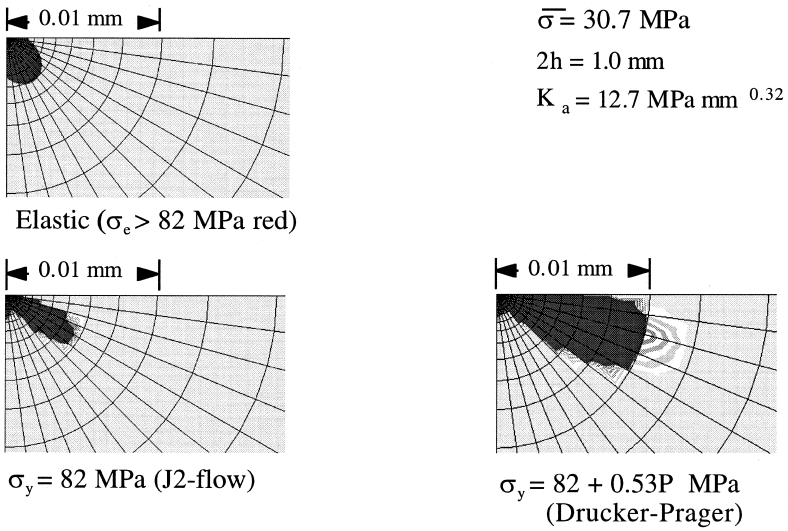

Fig. 8. Calculated interface corner yield zones when no interfacial crack is present. Dark gray in the plasticity calculations corresponds to an equivalent plastic strain > 0.0001.

accurate epoxy models of this type are not readily available. Nevertheless, simpler material models can be used to provide some insights. The crudest yield zone prediction shown in Fig. 8 uses a linear-elastic adhesive model to determine when the calculated effective stress exceeds the epoxy's yield strength. Also shown are results using a standard, elastic, perfectly-plastic J-2 flow theory and for an elastic, perfectly-plastic, Drucker–Prager model that incorporates a pressure-dependent yield strength. A realistic adhesive model should include pressure-dependent yielding since the 828/T403 epoxy used in the tests being modeled has a room temperature tensile yield strength of 70 MPa and a compressive yield strength of 100 MPa (at a strain rate of 0.0002/s, Reedy and Guess, 1996a). If a linear dependence on pressure P is assumed, $\sigma_y = 82 + 0.53$ P (MPa). Fig. 8 shows that the size and shape of the calculated yield zone is a strong function of which adhesive constitutive model is used. The calculated yield zone determined using elasticity and J-2 flow theory is in poor agreement with that determined when pressure-dependent yielding is included. The Drucker–Prager solution shows the largest yield zone, and the zone is shifted towards the interface. This is due to the presence of high levels of hydrostatic tension at the interface. Note that a slip line theory solution for a rigid, perfectly-plastic adhesive predicts a hydrostatic interfacial tension of 1.5 σ_y (Reedy and Guess, 1996b).

Fig. 9 plots the calculated interfacial normal stress for the J-2 flow and Drucker–Prager adhesive models along with interface corner singularity and perfectly-plastic slip line solutions. As observed previously, the interfacial normal stress is in good agreement with the singularity solution over a distance equal to 15% of the 1 mm thick bond. At this bond thickness the yield zone is deeply embedded within the region dominated by the singularity. Tests have been performed on joints as thin as 0.25 mm with good agreement with an interface corner failure analysis (Reedy and Guess, 1993). An interface corner failure analysis cannot, however, be applied to arbitrarily thin bonds. The region dominated by the singularity solution scales with bond thickness and shrinks as bond thickness is reduced. Ultimately it reaches a size comparable to that of the yield zone at joint failure.

One notable feature of the interface corner failure analysis is that is requires no detailed information about the failure process itself. Failure may be caused by a preexisting interfacial flaw or perhaps by a cavitation instability induced by the high levels of hydrostatic tension found at the interface. If an interfacial crack is present, it could be sharp, bridged, or have a yield zone comparable to its length. To

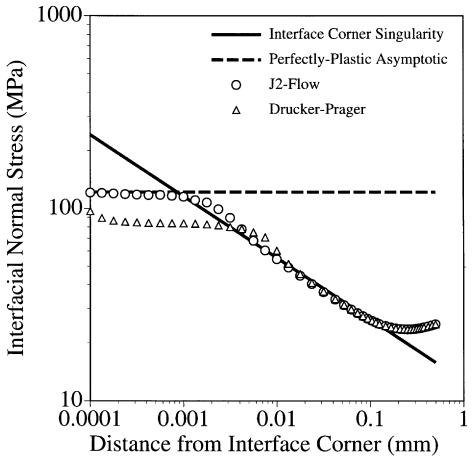

Fig. 9. Calculated interfacial normal stress when adhesive layer yields. Comparison with interface corner singularity and perfectly-plastic asymptotic solutions.

be applicable, it is only necessary that the failure process zone is deeply embedded within the region dominated by the interface corner singularity at failure.

Interfacial fracture mechanics is applicable when small-scale yielding conditions hold at the tip of a sharp, preexisting interfacial crack. In contrast to the interface corner failure analysis, the initial crack need not be small when compared to bond thickness. Indeed it might be easiest to apply this approach when the crack is long. When a steady-state cracking limit exists, the energy release rate is independent of crack length (e.g., eqn (13)). Consequently, one only needs to know that the crack is long, not its precise length. Failure occurs when the applied load generates an energy release rate larger than the interfacial toughness at the steady-state mode mixity.

Fig. 6 shows that in an adhesively-bonded butt joint with a short crack, G increases with increasing crack length. Therefore for a short crack, one must know the initial crack length to calculate the energy release rate G. Unfortunately it is often impractical or even impossible to routinely detect and measure the length of very small (e.g., 10 micron) interfacial flaws. It is also conceivable that joint failure does not initiate from a preexisting interfacial crack. Perhaps a flaw is generated in some way during loading. One would then need to know the size of the nucleated flaw and confirm that it is actually a sharp crack and not a localized zone of damaged material. Even if a short interfacial crack of known length does actually exist on the interface, other difficulties arise when applying an interfacial fracture mechanics approach. Tvergaard and Hutchinson (1994, 1996) have shown that adhesive ductility can cause interfacial toughness to increase rapidly as the crack initially extends until its length equals several bond thicknesses. Consequently, the application of interfacial fracture mechanics to an adhesively-bonded butt joint may necessitate the measurement of crack growth resistance. This measurement needs to be done at the relevant mode mixity and requires an accurate determination of changes in toughness during crack extension over a distance of the order of a bond thickness. Finally, it should again be emphasized that interfacial fracture mechanics requires that a sharp crack exists and that a small-scale yielding conditions applies. Only under these restrictive conditions and when small-scale interfacial cracking occurs, is interface corner toughness K_{ac} directly related to an interfacial toughness G_c by eqn (10).

Difficulties in rigorously applying interfacial fracture mechanics to adhesively-bonded joints with small flaws motivate the inherent flaw approach (Anderson and DeVries, 1987, 1989). The inherent flaw approach has pragmatic appeal. G_c is determined using a joint with an inserted crack of known length. This G_c is then used to infer the length of the inherent flaw a_0 that must exist for the fracture mechanics analysis to predict the measured joint strength when no flaw is inserted. There is a direct connection

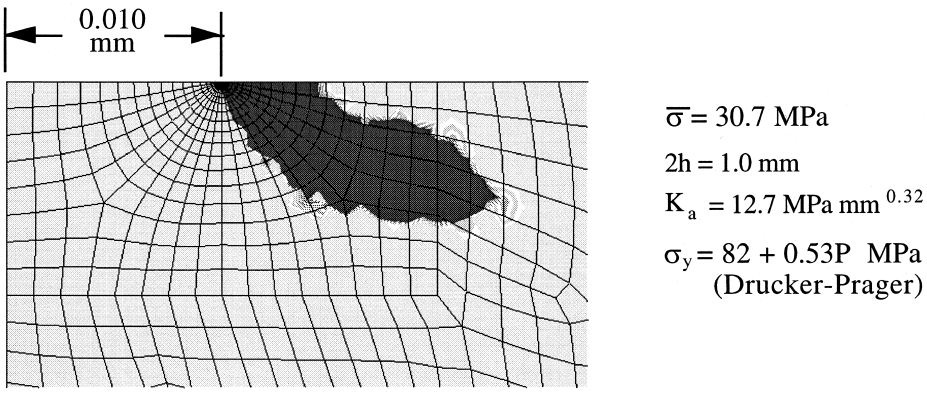

Fig. 10. Calculated yield zone at the tip of a short interfacial crack originating at the interface corner. Dark gray corresponds to an equivalent plastic strain > 0.0001.

between the interface corner failure analysis and the inherent flaw fracture mechanics analysis. Whenever failure occurs at a critical K_a value, the inherent flaw fracture mechanics approach can also be applied, and the predictions will be identical. All valid G_c, a_0 combinations must satisfy eqn (10), evaluated at K_{ac}. There is, of course, any number of valid G_c, a_0 pairs for a specified K_{ac}, and there is no reason to expect that a selected a_0, G_c pair is connected to a true crack. Indeed as noted above, when the interface corner failure analysis applies, there is no requirement that a sharp crack even exists.

Consider the application of the inherent flaw, interfacial fracture mechanics approach to an adhesively-bonded butt joint. Suppose one assumes that the joint contains a 0.01 mm long inherent flaw. An interfacial fracture analysis using $a_0 = 0.01$ mm will be equilvalent to an interface corner failure analysis with $K_{ac} = 12.7$ MPa mm$^{0.32}$, provided that G_c is set equal to 21.4 J/m^2 (eqn (10), $E = 3.5$ GPa, $\nu = 0.35$). This choice of a_0 and G_c will predict the same variation in joint strength with bond thickness as an interface corner analysis using $K_{ac} = 12.7$ MPa mm$^{0.32}$. A full finite element analysis of a joint containing a 0.01 mm long crack shows that there is significant crack-tip yielding when $\bar{\sigma} = 30.7$ MPa (Fig. 10, using the Drucker–Prager adhesive model). Note that this load level corresponds to

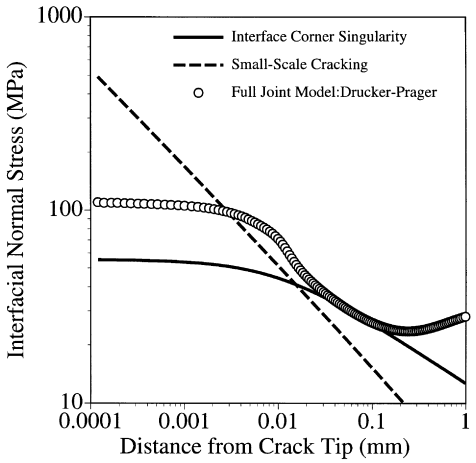

Fig. 11. Calculated interfacial normal stress for a 0.01 mm long interfacial crack originating at the interface corner when the adhesive yields. Comparison with interface corner singularity and small-scale cracking solutions.

$G = 21.4$ J/m^2 (eqn (12)). The calculated yield zone is about the same length as the crack. At joint failure small-scale yielding conditions do not apply when the crack is 0.01 mm long. An independent measurement of the interfacial toughness, conducted in a manner that generates small-scale yielding (e.g., using a DCB specimen with a long initial crack), would measure a different toughness value. There is no direct connection between the G_c toughness value used in conjunction with an inherent flaw of 0.01 mm and the interfacial toughness measured under small-scale yielding conditions. Fig. 11 plots the calculated interfacial normal stress along with the small-scale cracking and the interface corner singularity solutions. The results for the full joint model show that the yield zone is deeply embedded within the interface corner singularity solution. This indicates that the interface corner failure analysis should be applicable. On the other hand, the small-scale cracking solution does not merge with the full joint solution. Extensive crack-tip yielding perturbs the solution to the extent that the small-scale cracking solution no longer describes the asymptotic behavior. An inherent flaw fracture analysis based on fracture parameters $a_0 = 0.01$ mm and $G_c = 21.4$ J/m^2 will predict the observed variation in joint strength with bond thickness, but these parameters lack physical significance. This analysis applies only because the choice of fracture parameters is equivalent to $K_{ac} = 12.7$ MPa mm$^{0.32}$.

5. Conclusion

Interfacial crack growth from the interface corner of a tensile-loaded, adhesively-bonded butt joint with rigid adherends has been analyzed. Asymptotic solutions for both small-scale cracking and steady-state cracking are presented. The asymptotic results for energy release rate and mode mixity form a reasonably tight envelope of values determined by a full finite element analysis of a joint with an interfacial crack that is varied from 0.001 to 10 times the bond thickness. An interface corner failure analysis is applicable only when unstable crack growth initiates from a fracture process zone that is deeply embedded within the region dominated by the interface corner singularity. Interfacial fracture mechanics is strictly applicable only when small-scale yielding conditions hold at the tip of a sharp, preexisting interfacial crack. A rigorous application of interfacial fracture mechanics to short cracks is difficult because one must independently measure the initial crack length and also crack growth resistance data. For this reason the inherent flaw approach has pragmatic appeal. The small-scale cracking solution indicates that when one can apply an interface corner failure analysis, one can also apply an interfacial fracture mechanics analysis with a suitably chosen inherent flaw. Although the two methods are equivalent, it should be emphasized that the inherent flaw and corresponding toughness may have limited physical significance.

Acknowledgements

This work was performed at Sandia National Laboratories. Sandia is a multiprogram laboratory operated by Sandia Corporation, a Lockheed Martin Company, for the United States Department of Energy under Contract DE-AC04-94AL85000.

References

Akisanya, A.R., Fleck, N.A., 1997. Interfacial cracking from the free-edge of a long bi-material strip. International Journal of Solids and Structures 33, 1645–1665.

Anderson, G.P., DeVries, K.L., 1987. Predicting bond strength. Journal of Adhesion 23, 289–302.

Anderson, G.P., DeVries, K.L., 1989. Predicting strength of adhesive joints from test results. International Journal of Fracture 39, 191–200.

Bogy, D.B., 1968. Edge-bonded dissimilar orthogonal elastic wedges under normal and shear loading. Journal of Applied Mechanics 35, 460–466.

Bogy, D.B., 1970. On the problem of edge-bonded elastic quarter-planes loaded at the boundary. International Journal of Solids and Structures 6, 1287–1313.

Chen, D.H., 1994. Analysis of singular stress field around the inclusion corner tip. Engineering Fracture Mechanics 49, 533–546.

Ding, S., Meekisho, L., Kumosa, M., 1994. Analysis of stress singular fields at a bimaterial wedge corner. Engineering Fracture Mechanics 49, 569–585.

Dundurs, J., 1969. Discussion of edge-bonded dissimilar orthogonal elastic wedges under normal and shear loading. Journal of Applied Mechanics 36, 650–652.

Dunn, M.L., Suwito, W., Cunningham, S., 1997a. Fracture initiation at sharp notches: correlation using critical stress intensities. International Journal of Solids and Structures 34, 3873–3883.

Dunn, M.L., Suwito, W., Cunningham, S., May, C.W., 1997b. Fracture initiation at sharp notches under mode I, mode II and mild mixed mode loading. International Journal of Fracture 84, 367–381.

Gradin, P.A., 1982. A fracture criterion for edge-bonded bimaterial bodies. Journal of Composite Material 16, 448–456.

Grenestedt, J.L., Hallstrom, S., 1997. Crack initiation from homogeneous and bimaterial corners. Journal of Applied Mechanics 64, 811–818.

Groth, H.L., 1988. Stress singularities and fracture at interface corners in bonded joints. International Journal of Adhesion and Adhesives 8, 107–113.

Hattori, T., Sakata, S., Murakami, G., 1989. A stress singularity parameter approach for evaluating the interfacial reliability of plastic encapsulated LSI devices. Journal of Electronic Packaging 111, 243–248.

Hutchinson, J.W., Suo, Z., 1992. Mixed mode cracking in layered materials. Advances in Applied Mechanics 29, 63–191.

Matos, P.P.L., McMeeking, R.M., Charalambides, P.G., Drory, M.D., 1989. A method for calculating stress intensities in bimaterial fracture. International Journal of Fracture 40, 235–254.

Munz, D., Yang, Y.Y., 1992. Stress singularities at the interface in bonded dissimilar materials under mechanical and thermal loading. Journal of Applied Mechanics 59, 857–861.

Reedy Jr., E.d., 1990. Intensity of the stress singularity at the interface corner between a bonded elastic and rigid layer. Engineering Fracture Mechanics 36, 575–583.

Reedy Jr., E.D., 1993. Asymptotic interface corner solutions for butt tensile joints. International Journal of Solids and Structures 30, 767–777.

Reedy Jr., E.D., Guess, T.R., 1993. Comparison of butt tensile strength data with interface corner stress intensity factor prediction. International Journal of Solids and Structures 30, 2929–2936.

Reedy Jr., E.D., Guess, T.R., 1995. Butt joint tensile strength: interface corner stress intensity factor prediction. Journal of Adhesion Science and Technology 9, 237–251.

Reedy Jr., E.D., Guess, T.R., 1996a. Butt joint strength: effect of residual stress and stress relaxation. Journal of Adhesion science and Technology 10, 33–45.

Reedy Jr., E.D., Guess, T.R., 1996b. Interface corner stress states: plasticity effects. International Journal of Fracture 81, 269–282.

Reedy Jr., E.D., Guess, T.R., 1997. Interface corner failure analysis of joint strength: effect of adherend stiffness. International Journal of Fracture 88, 305–314.

Rice, J.R., 1968. A path independent integral and the approximate analysis of strain concentration by notches and cracks. Journal of Applied Mechanics 35, 379–386.

Rice, J.R., 1988. Elastic fracture mechanics concepts for interfacial cracks. Journal of Applied Mechanics 55, 98–103.

Szabó, B.A., Yosibash, Z., 1996. Numerical analysis of singularities in two dimensions. Part 2: computation of generalized flux/stress intensity factors. International Journal for Numerical Methods in Engineering 39, 409–434.

Tvergaard, V., Hutchinson, J.W., 1994. Toughness of an interface along a thin ductile layer joining elastic solids. Philosophical Magazine A 70, 641–656.

Tvergaard, V., Hutchinson, J.W., 1996. On the toughness of ductile adhesive joints. Journal of the Mechanics and Physics of Solids 44, 789–800.

Williams, M.L., 1952. Stress singularities resulting from various boundary conditions in angular corners of plates in extension. Journal of Applied Mechanics 19, 526–528.